

# H<sub>5</sub>PV<sub>2</sub>Mo<sub>10</sub>O<sub>40</sub> Polyoxometalate Encapsulated in NU-1000 Metal–Organic Framework for Aerobic Oxidation of a Mustard Gas Simulant

Cassandra T. Buru, Megan C. Wasson, Omar K. Farha\*

International Institute of Nanotechnology and Department of Chemistry, Northwestern University, 2145 Sheridan Road, Evanston, Illinois 60208, USA

\* Email: o-farha@northwestern.edu

## Table of Contents

|   |            |
|---|------------|
| Section S1. <b>Materials and Physical Methods</b> ..... | <b>S2</b>  |
| Section S2. <b>Composite Characterization</b> .....     | <b>S3</b>  |
| Section S3. <b>Catalytic Studies</b> .....              | <b>S7</b>  |
| Section S4. <b>References</b> .....                     | <b>S11</b> |

## Section S1. Physical Methods

The supercritical drying process used a Tousimis™ Samdri PVT-3D critical point drier in which liquid CO<sub>2</sub> was used to exchange ethanol 4 times over 8 h. The material was then heated above 31 °C (P = 73 atm), the critical point of CO<sub>2</sub> before the instrument was evacuated at a rate of 0.1 sccm.<sup>1-3</sup>

All MOF samples were activated by exposure of 20 to 100 mg of material for 12 hours under high vacuum on a Micromeritics Smart VacPrep instrument. N<sub>2</sub> adsorption and desorption isotherm measurements were performed on a Micromeritics Tristar II at 77 K. DFT calculated pore size distributions used the slit geometry and the N<sub>2</sub> @ 77 on carbon slit pores by NLDFT kernel.

Inductively coupled plasma optical emission spectroscopy (ICP-OES) samples of solids were prepared in a 2-5 mL Biotage microwave vial by dissolving 1-2 mg of sample in 5 drops of H<sub>2</sub>SO<sub>4</sub> and slowly adding 2 mL of HNO<sub>3</sub>. The vial was cringe-capped and heated to 150 °C for 15 min in a SPX microwave reactor. The resulting orange-yellow solution was made colorless by adding 0.5 mL H<sub>2</sub>O<sub>2</sub> (30 wt% in water) and heating in a sand bath for 10 min. To the colorless or pale solution, 10 mL of deionized water was added, and the resulting dilution analyzed with Thermo iCap7600 ICP-OES spectrometer, equipped with a CCD detector and Ar plasma covering 175-785 nm range.

Powder X-ray diffraction (PXRD) patterns were collected on a Stoe STADI-P instrument. Samples were using K $\alpha$ 1 Cu radiation, a step size of  $2\theta = 0.015^\circ$  over a  $2\theta$  range of 1 to 25°. Variable temperature powder X-ray diffraction (PXRD) patterns were collected on a Stoe STADI-MP instrument equipped with a furnace using K $\alpha$ 1 Mo radiation.

Solution NMR spectra were collected on a 400 MHz Agilent DD MR-400 system at IMSERC (Integrated Molecular Structure Education and Research Center) at Northwestern University. Solid-state NMR spectra were collected on a Bruker 400 MHz NMR system spinning at 10,000 Hz.

Scanning electron microscopy (SEM) images and energy dispersive spectroscopy (EDS) line scans were collected using a Hitachi SU8030 FE-SEM microscope at Northwestern University's EPIC/NUANCE facility. All samples were coated with ~15 nm of OsO<sub>4</sub> immediately prior to imaging.

GC-FID measurements were carried out on an Agilent Technologies 7820A GC system equipped with an Agilent J&W GC HP-5 capillary column (30 m  $\times$  320  $\mu$ m  $\times$  0.25  $\mu$ m film thickness). All samples were filtered and diluted with dichloromethane prior to injection. Starting temperature: 70 °C, Hold: 0.5 min, Ramp: 30 °C/min, Time: 1 min, Ramp: 75 °C/min, End temperature: 250 °C.

Thermogravimetric analyses (TGA) were performed on a Mettler Toledo STAR® TGA/DSC 1 under a N<sub>2</sub> flow at a 10 °C/min ramp rate from 25 to 700 °C. For TGA-MS measurements, a Netzsch Simultaneous Thermal Analysis (STA 449F3) instrument coupled to a GC-MS was used.

X-ray photoelectron spectroscopy measurements were carried out on a Thermo Scientific ESCALAB 250 Xi equipped with an electron flood gun and a scanning ion gun. Analysis used the Thermo Scientific Advantage Data System software, and C1s peak (284.8 eV) peak was used as the reference. Oxidation states of Mo and V were assigned by comparison to previously published data.<sup>4,5</sup>

## Section S2. Composite Characterization

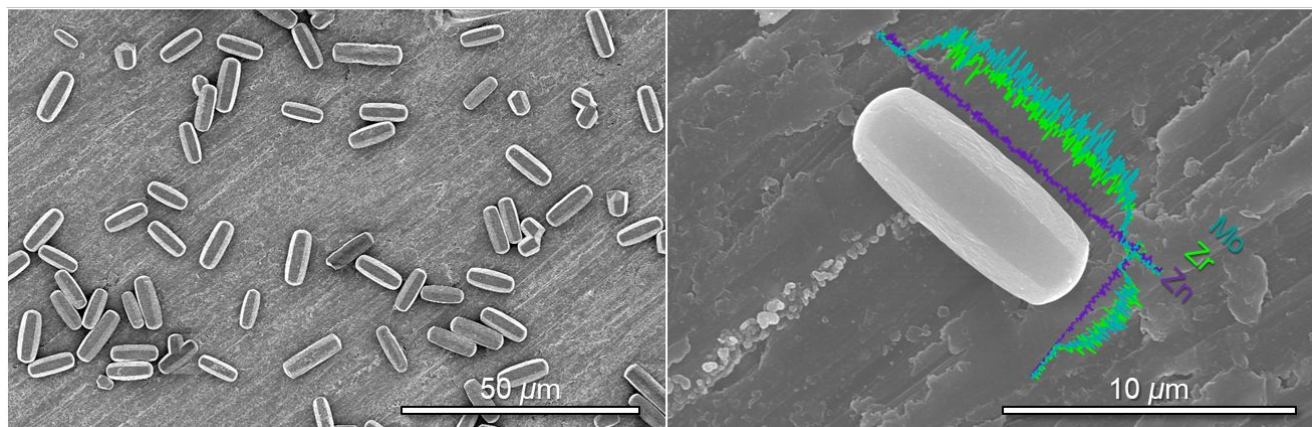


**Figure S1.** SEM images of NU-1000 before (left) and after (right)  $[\text{PV}_2\text{Mo}_{10}\text{O}_{40}]^{5-}$  incorporation. EDS line scans of Mo and Zr compared to baseline Zn.

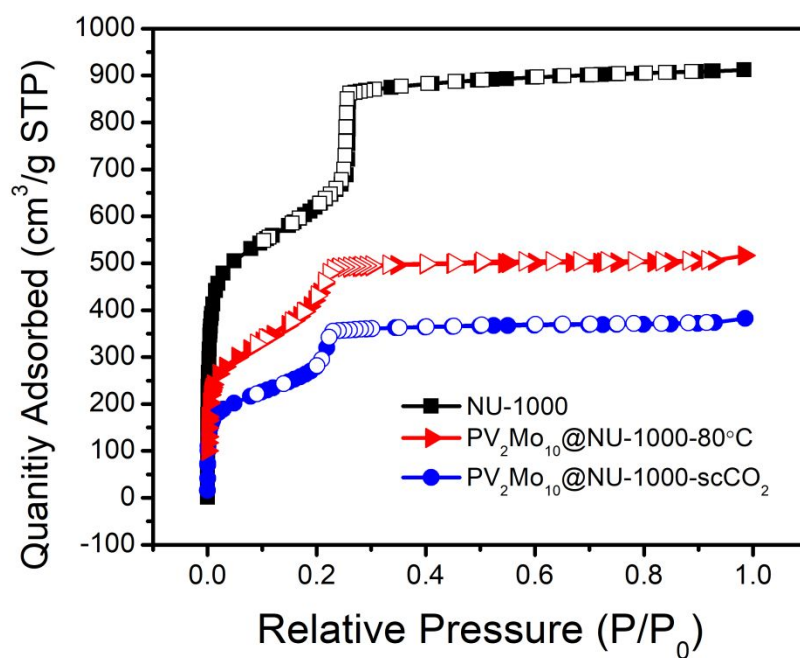


**Figure S2.** Gravimetric  $\text{N}_2$  adsorption (filled) and desorption (unfilled) isotherms for NU-1000 and composites with  $[\text{PV}_2\text{Mo}_{10}\text{O}_{40}]^{5-}$ .

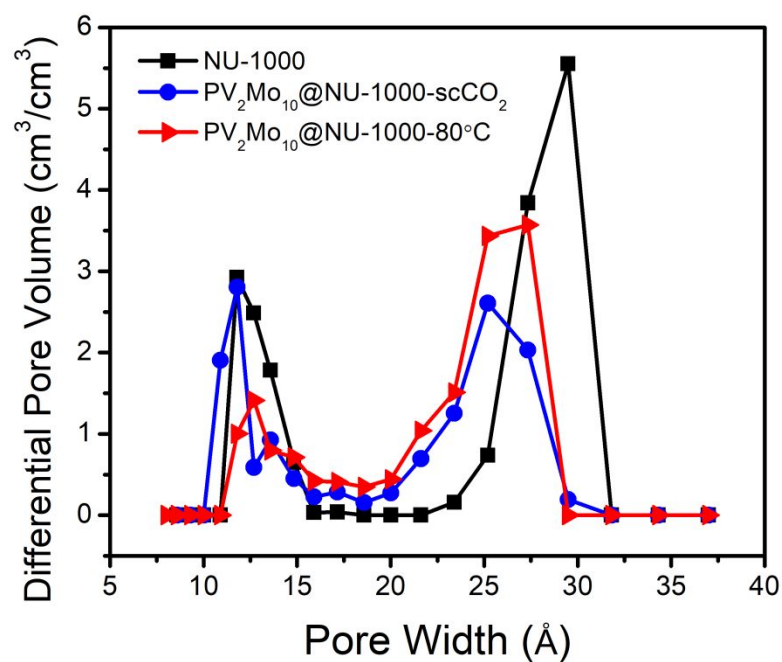


**Figure S3.** Volumetric DFT-calculated pore size distributions of NU-1000 and  $\text{PV}_2\text{Mo}_{10}@ \text{NU-1000}$ .

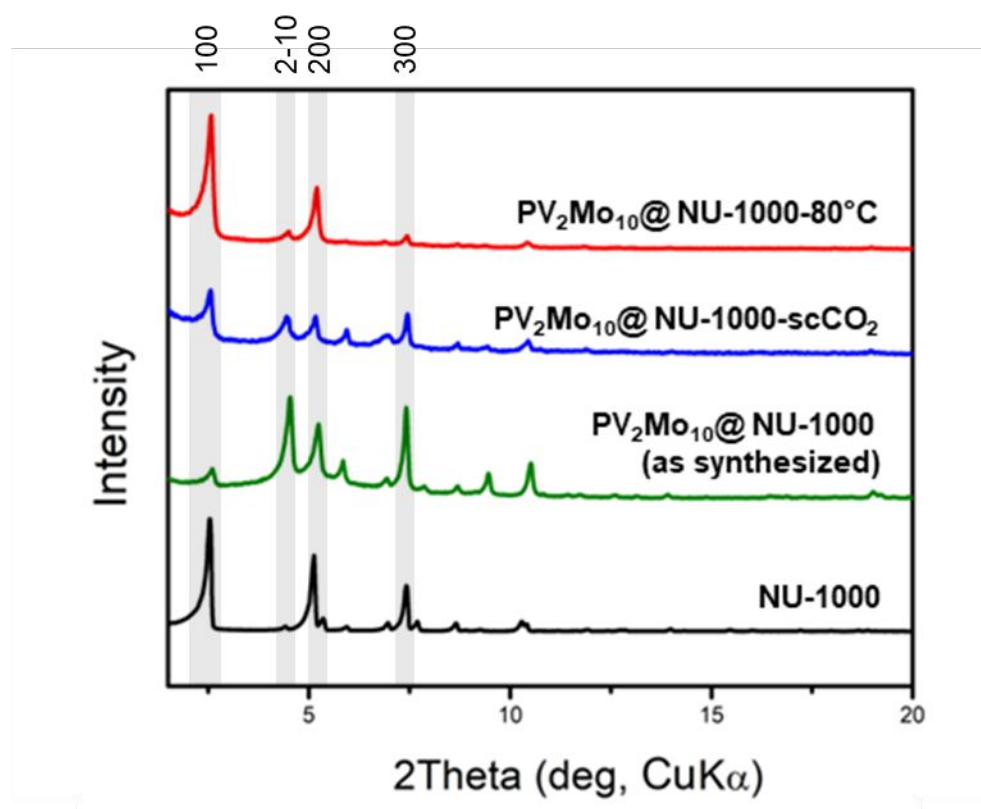


**Figure S4.** Indexed PXRD patterns of NU-1000,  $\text{PV}_2\text{Mo}_{10}@ \text{NU-1000-scCO}_2$ , and  $\text{PV}_2\text{Mo}_{10}@ \text{NU-1000-80}^\circ\text{C}$ .

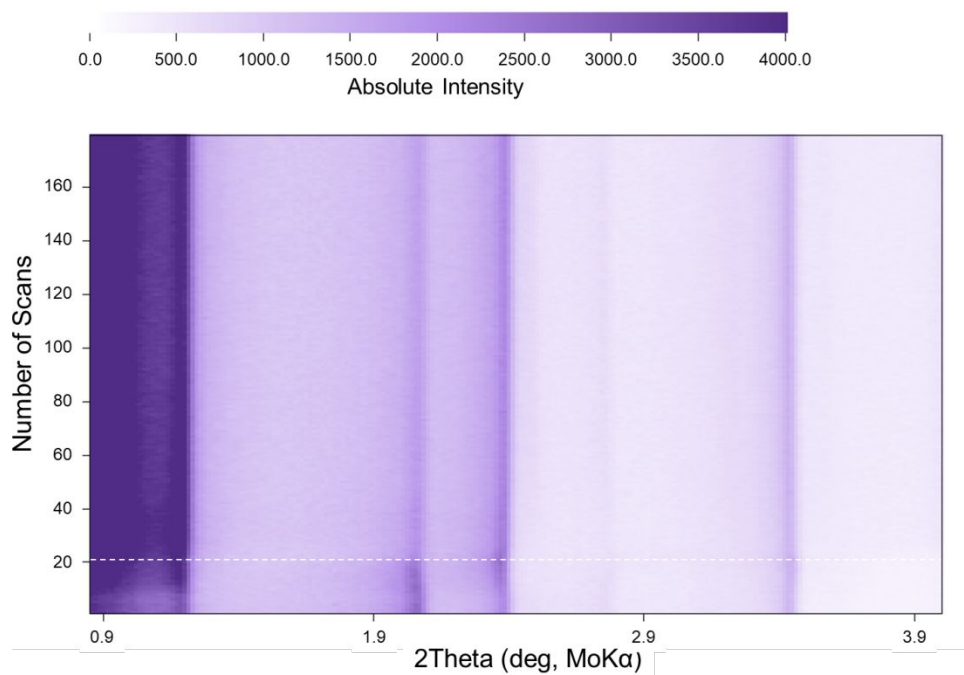


**Figure S5.** *In situ* variable temperature PXRD patterns for  $\text{PV}_2\text{Mo}_{10}\text{@NU-1000-scCO}_2$ . N (y-axis) indicates the number of scans taken at 80 °C. Each scan is 1 min apart. The horizontal dotted white line highlights where the structural change occurs.

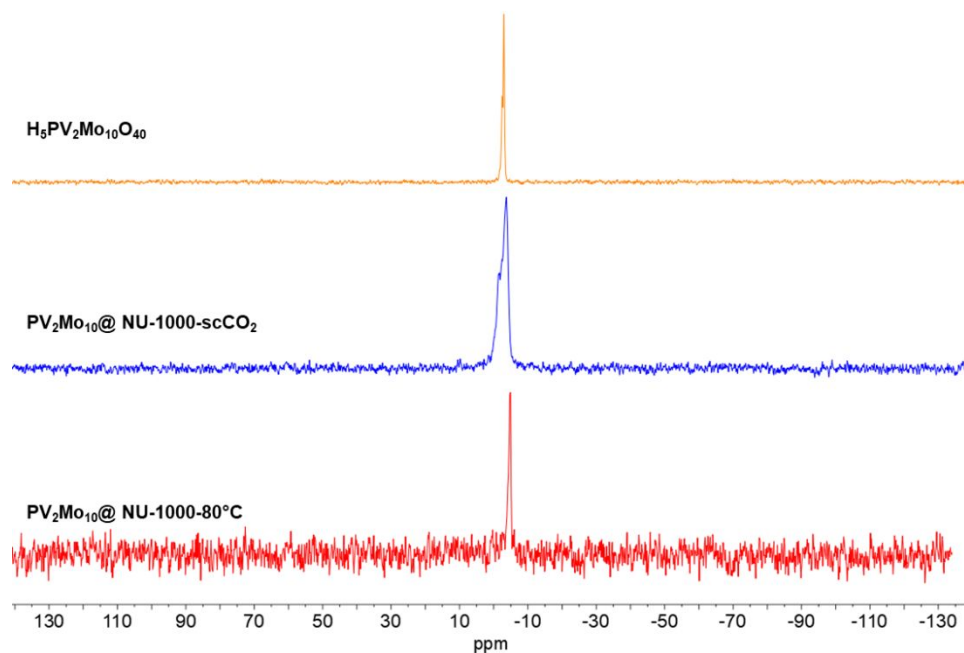


**Figure S6.**  $^{31}\text{P}$  CPMAS NMR spectra of  $\text{H}_5\text{PV}_2\text{Mo}_{10}\text{O}_{40}$  and  $\text{PV}_2\text{Mo}_{10}\text{@NU-1000}$ .

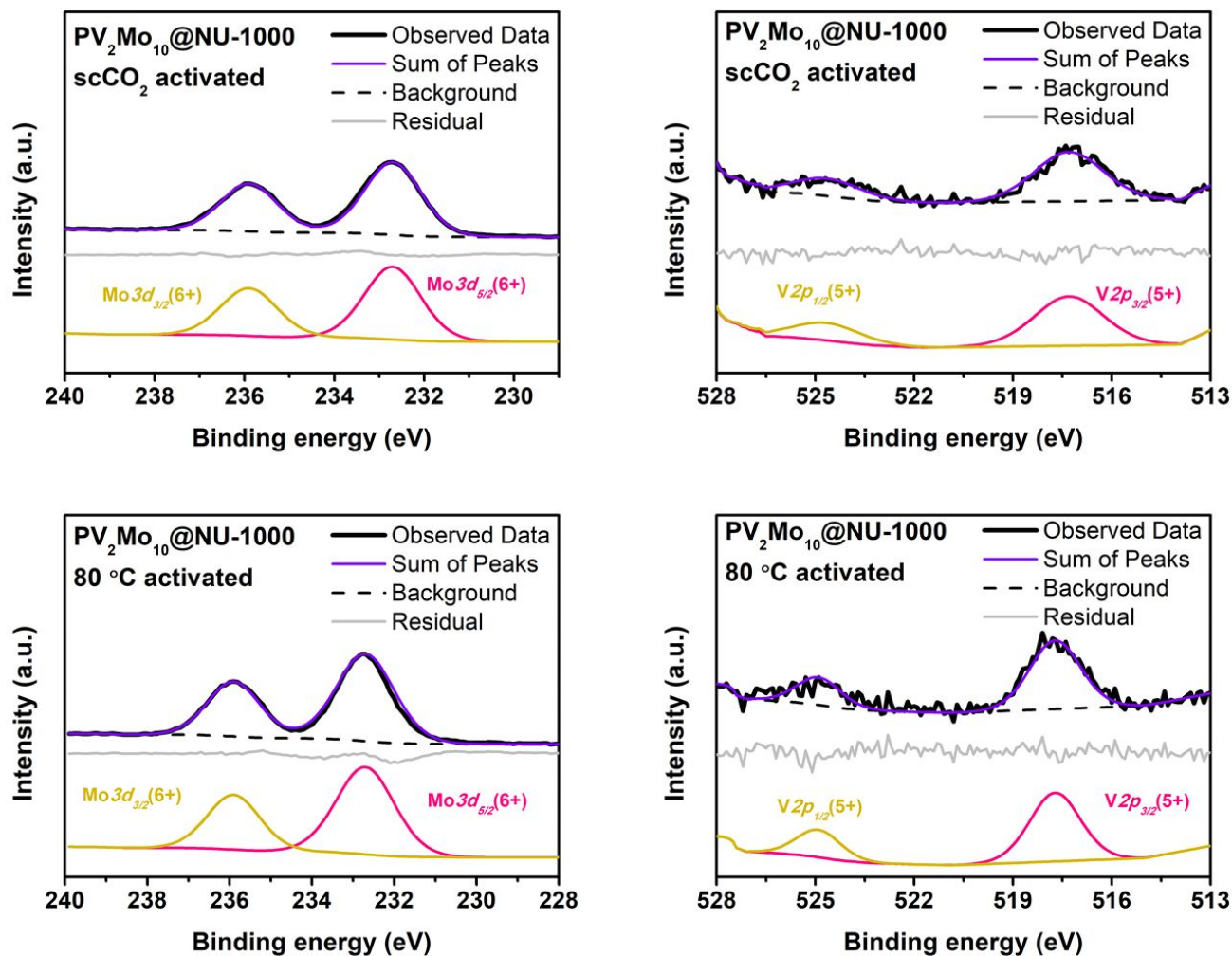


**Figure S7.** XPS spectra of  $\text{PV}_2\text{Mo}_{10}\text{@NU-1000-scCO}_2$  (top) and  $\text{PV}_2\text{Mo}_{10}\text{@NU-1000-80}^\circ\text{C}$  (bottom) for Mo (left) and V (right).



## Section S3. Catalytic Studies

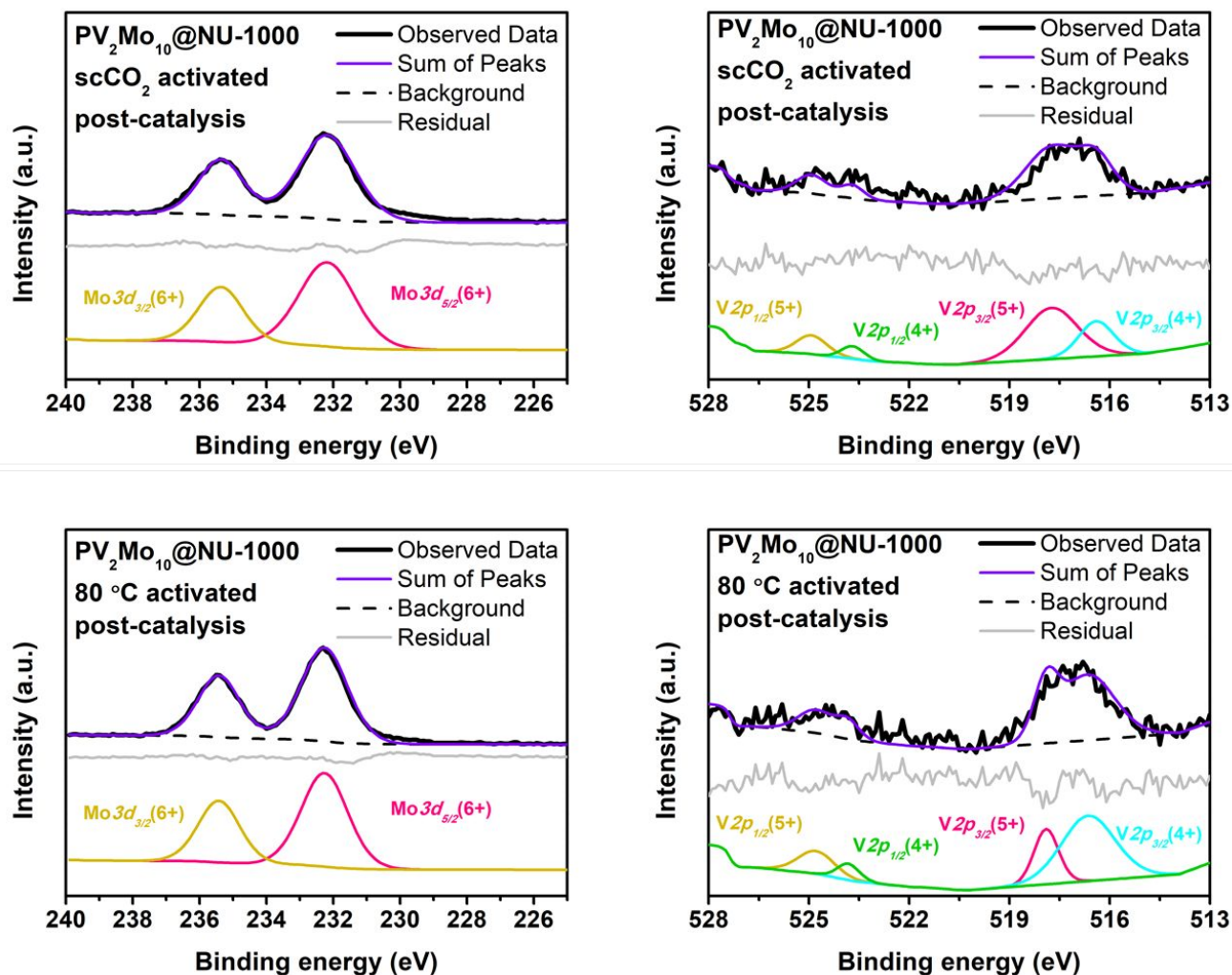


**Figure S8.** XPS spectra of PV<sub>2</sub>Mo<sub>10</sub>@NU-1000-scCO<sub>2</sub> (top) and PV<sub>2</sub>Mo<sub>10</sub>@NU-1000-80 °C (bottom) **after catalysis** for Mo (left) and V (right). Note, that the POMs were not kept rigorously under air-free conditions post-catalysis and could have partially oxidized V.

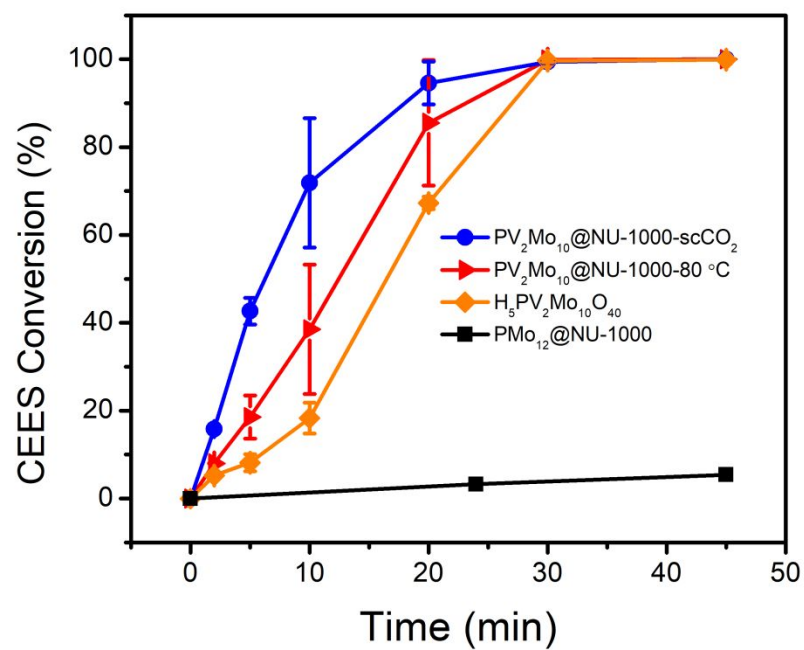


**Figure S9.** The kinetic traces with error bars of each material used for reaction (Figure 3A). Catalyst is normalized to the number of POM clusters, the reductant is isobutyraldehyde, 1 mL cyclohexane was used as solvent. Traces are averages of at least 3 trials. Error bars represent 1 standard deviation.



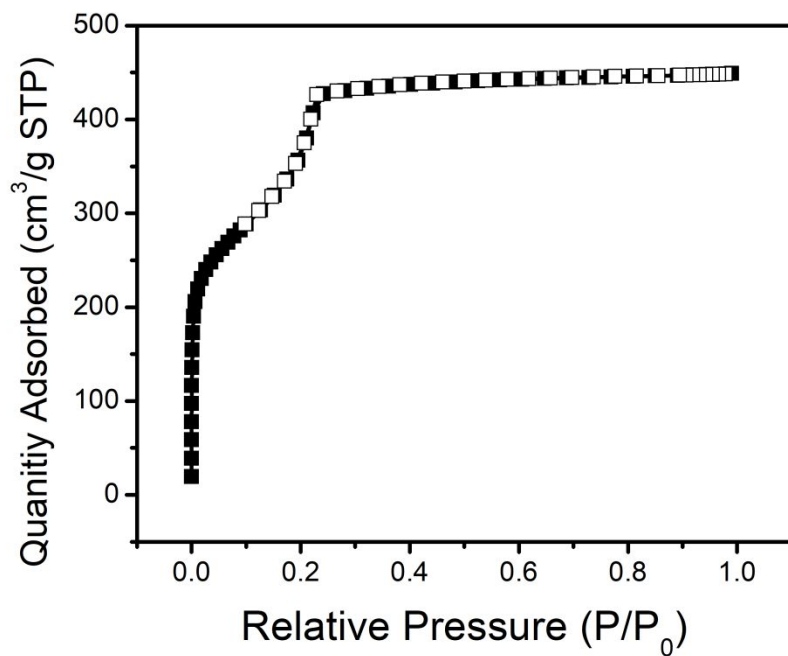


**Figure S10.** Gravimetric N<sub>2</sub> adsorption (filled) and desorption (unfilled) isotherms for PMo<sub>12</sub>@NU-1000 after scCO<sub>2</sub> activation (BET: 1450 m<sup>2</sup>/g).

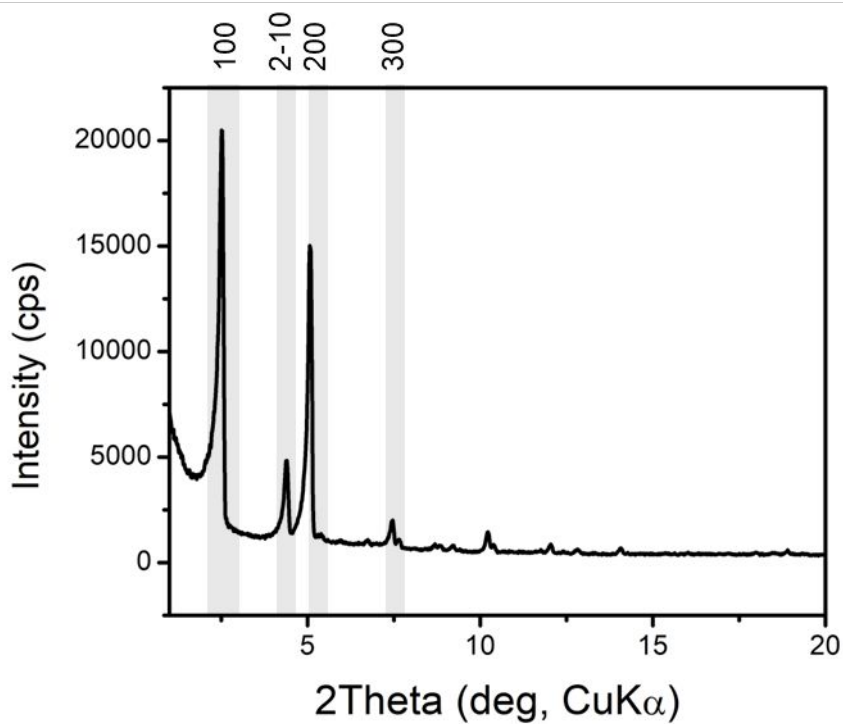


**Figure S11.** Indexed PXRD pattern for PMo<sub>12</sub>@NU-1000 after scCO<sub>2</sub> activation showing POMs primarily located in micropores.

**Table S1.** Reaction conditions tuning amount of reductant, temperature, atmosphere, and solvent collected at 45 min.

| Catalyst   | Reductant   | Temperature | Atmosphere           | Solvent             | Conversion |
|--|-------------|-------------|----------------------|---------------------|------------|
|  | t           | (°C)        |                      |                     | (%)        |
| H <sub>5</sub> PV <sub>2</sub> Mo <sub>10</sub> O <sub>40</sub>          | 5 eq        | 70          | O <sub>2</sub>       | Cyclohexane         | 100        |
| H <sub>5</sub> PV <sub>2</sub> Mo <sub>10</sub> O <sub>40</sub>          | 5 eq        | 70          | <b>Air</b>           | Cyclohexane         | 23         |
| H <sub>5</sub> PV <sub>2</sub> Mo <sub>10</sub> O <sub>40</sub>          | 5 eq        | 70          | <b>N<sub>2</sub></b> | Cyclohexane         | <1         |
| H <sub>5</sub> PV <sub>2</sub> Mo <sub>10</sub> O <sub>40</sub>          | <b>2 eq</b> | 70          | O <sub>2</sub>       | Cyclohexane         | 27         |
| H <sub>5</sub> PV <sub>2</sub> Mo <sub>10</sub> O <sub>40</sub>          | <b>1 eq</b> | 70          | O <sub>2</sub>       | Cyclohexane         | 3          |
| H <sub>5</sub> PV <sub>2</sub> Mo <sub>10</sub> O <sub>40</sub>          | <b>0 eq</b> | 70          | O <sub>2</sub>       | Cyclohexane         | 1          |
| H <sub>5</sub> PV <sub>2</sub> Mo <sub>10</sub> O <sub>40</sub>          | 5 eq        | <b>22</b>   | O <sub>2</sub>       | Cyclohexane         | 14         |
| H <sub>5</sub> PV <sub>2</sub> Mo <sub>10</sub> O <sub>40</sub>          | 5 eq        | 70          | O <sub>2</sub>       | <b>Acetonitrile</b> | 9          |
| H <sub>3</sub> Mo <sub>12</sub> O <sub>40</sub>                          | 5 eq        | 70          | O <sub>2</sub>       | Cyclohexane         | 4          |
| NU-1000  | 5 eq        | 70          | O <sub>2</sub>       | Cyclohexane         | <1         |
| PMo <sub>12</sub> @NU-1000   | 5 eq        | 70          | O <sub>2</sub>       | Cyclohexane         | 5          |
| PV <sub>2</sub> Mo <sub>10</sub> @NU-1000-scCO <sub>2</sub>              | 5 eq        | 70          | O <sub>2</sub>       | Cyclohexane         | 100        |
| PV <sub>2</sub> Mo <sub>10</sub> @NU-1000-80°C                           | 5 eq        | 70          | O <sub>2</sub>       | Cyclohexane         | 100        |
| Recycled PV <sub>2</sub> Mo <sub>10</sub> @NU-1000                       | 5 eq        | 70          | O <sub>2</sub>       | Cyclohexane         | 100        |
| Recycled H <sub>5</sub> PV <sub>2</sub> Mo <sub>10</sub> O <sub>40</sub> | 5 eq        | 70          | O <sub>2</sub>       | Cyclohexane         | 5          |

## Section S4. References

- (1) Nelson, A. P.; Farha, O. K.; Mulfort, K. L.; Hupp, J. T. Supercritical Processing as a Route to High Internal Surface Areas and Permanent Microporosity in Metal - Organic Framework Materials. *J. Am. Chem. Soc.* **2009**, *131*, 458–460.
- (2) Farha, O. K.; Shultz, A. M.; Sarjeant, A. A.; Nguyen, S. T.; Hupp, J. T. Active-Site-Accessible, Porphyrinic Metal À Organic Framework Materials. *J. Am. Chem. Soc.* **2011**, *133*, 5652–5655.
- (3) Shultz, A. M.; Farha, O. K.; Adhikari, D.; Sarjeant, A. A.; Hupp, J. T.; Nguyen, S. T. Selective Surface and Near-Surface Modification of a Noncatenated, Catalytically Active Metal-Organic Framework Material Based on Mn(salen) Struts. *Inorg. Chem.* **2011**, *50*, 3174–3176.
- (4) Silversmit, G.; Depla, D.; Poelman, H.; Marin, G. B.; De Gryse, R. Determination of the V2p XPS binding energies for different vanadium oxidation states (V5+ to V0+). *J. Electron Spectros. Relat. Phenomena* **2004**, *135* (2–3), 167–175.
- (5) Choi, J.-G.; Thompson, L. T. XPS study of as-prepared and reduced molybdenum oxides. *Appl. Surf. Sci.* **1996**, *93* (2), 143–149.